RSC Advances

PAPER

View Article Online
View Journal | View Issue

Cite this: *RSC Adv.*, 2026, **16**, 17063

Synthesis and application of polyoxometalate ionic liquid-coated ZnO nanoflowers for efficient extraction of tetracycline residues in food and environmental samples

Zahra Nazar,[af] Mohannad Al-Hmoud,[b] Zahra Mohammadizadeh Tahroudi,[a] Alexandra Suvorova,[a] Muhammad Salman Khan, *[c] Ayed M. Binzowaimil,[b] Hijaz Ahmad[d] and Ahmad Irfan[e]

Monitoring of antibiotic residues in foodstuffs is essential to ensure consumer safety. Among these antibiotics, tetracyclines (TCs) are the most widely used veterinary drugs, and their residues pose serious health risks. A novel sorbent material consisting of zinc oxide modified with a polyoxometalate-based ionic liquid (POM-IL@ZnO) was applied in dispersive micro-solid phase extraction (D-μSPE) coupled with high-performance liquid chromatography-ultraviolet detection (HPLC-UV) for the determination of tetracyclines, namely oxytetracycline (OTC), tetracycline (TC), and chlortetracycline (CTC), in complex food and water samples. The morphology, crystallinity, thermal stability, and structural characteristics of POM-IL@ZnO were characterized using scanning electron microscopy (SEM), powder X-ray diffraction (PXRD), thermogravimetric analysis (TGA), and Fourier-transform infrared spectroscopy (FTIR). Systematic optimization was performed by evaluating key extraction parameters, including sorbent recyclability, eluent type and volume, extraction time, pH, and adsorbent amount. The developed method achieved maximum recoveries of 99.8%, low limits of detection (0.026–0.067 μg mL^{-1}) and quantification (0.080–0.210 μg mL^{-1}), excellent linearity ($R^2 \geq 0.998$), a linear range of 10–1000 μg mL^{-1}, and relative standard deviation (RSD) values ranging from 1.8% to 6.0%. The POM-IL@ZnO sorbent-based D-μSPE method demonstrates strong potential for routine food safety analysis as a rapid, sensitive, and environmentally friendly approach for determining tetracycline residues. The performance of the developed method was compared with previously reported SPE-based methods.

Received 21st January 2026
Accepted 21st March 2026

DOI: 10.1039/d6ra00560h

rsc.li/rsc-advances

1. Introduction

The presence of pharmaceutical residues in foodstuffs and environmental samples has become a global concern due to their potential impacts on ecological stability and human health. Tetracyclines (TCs), including oxytetracycline (OTC), tetracycline (TC), and chlortetracycline (CTC), are widely used antimicrobials in both human and veterinary medicine.[1] However, their extensive and often uncontrolled use has led to frequent detection in milk, honey, and wastewater as environmental contaminants.[2] The environmental persistence of TCs disrupts microbial ecology and promotes the emergence of antibiotic-resistant bacteria, posing serious risks to global public health. Despite these hazards, regulatory limits for acceptable concentrations of TCs in environmental matrices remain inadequately defined. In animal-derived food products, TC residues may cause allergic reactions, gastrointestinal disturbances, immunological imbalances, and potential carcinogenic effects.[3] The European Union has established maximum residue limits (MRLs) of 100 μg kg^{-1} for TCs in foodstuffs.[4] The analysis of TC residues in animal-derived food products requires an effective analytical method for food safety assessment. TCs have been determined using various analytical techniques, including spectrophotometry,[5] fluorescence detection, chromatographic,[6] and electrochemical methods.[7] Due to their trace concentrations and high polarity in complex matrices, appropriate sample preparation procedures, particularly extraction techniques, are necessary before instrumental analysis.[8] These pre-treatment methods enable analyte

[a]*School of Molecular Sciences, University of Western Australia, Australia*
[b]*Department of Physics, College of Science, Imam Mohammad Ibn Saud Islamic University (IMSIU), Riyadh, 13318, Saudi Arabia*
[c]*Department of Physics, Abdul Wali Khan University, Mardan, 23200, Pakistan. E-mail: salmankhan73030@gmail.com*
[d]*Irfan Suat Gunsel Operational Research Institute, Near East University, Nicosia/TRNC, 99138 Mersin 10, Turkey*
[e]*Department of Chemistry, College of Science, King Khalid University, P.O. Box 9004, 61413, Abha, Saudi Arabia*
[f]*Institute of Chemical Sciences, Bahauddin Zakariya University, Multan, 60800, Punjab, Pakistan*

enrichment and minimize matrix interference,[9] especially in complex samples such as milk and honey. High-performance liquid chromatography (HPLC) is a widely used separation technique for the analysis of compounds with diverse physicochemical properties and is commonly applied for the detection of TCs in environmental and food samples.[10] TCs have been separated and preconcentrated using conventional techniques such as liquid–liquid extraction (LLE),[11] solid-phase extraction (SPE),[12] solid-phase microextraction (SPME),[13] single-drop microextraction (SDME),[14] and dispersive liquid–liquid microextraction (DLLME). Dispersive solid-phase extraction (D-SPE) is a versatile modification of SPE that offers a simple, rapid, and efficient extraction procedure. Various sorbent materials have been developed for the extraction of TCs. These include conventional adsorbents such as molecularly imprinted polymers,[15] nano-fibers,[16] nanotubes,[17] graphene oxide, and metal–organic frameworks (MOFs).[18] Despite their high surface area and tunable interactions, these materials still present limitations related to cost, reusability, and selectivity. Polyoxometalates (POMs) are nanoscale clusters of inorganic transition metal–oxide units that have attracted considerable attention due to their structural, catalytic, electrochemical, and biological properties.[19] Research on POMs has advanced rapidly since Pope and Müller reported the remarkable properties and potential applications of these metal–oxide complexes in the early 1990s.[20] In recent years, POMs have been extensively utilized in the development of functional materials and nanosystems for biomedical applications and electrocatalysis.[21]

Polyoxometalate-based ionic liquids (POM-ILs), in which bulky organic cations (*e.g.*, ammonium or phosphonium cations) are combined with molecular metal–oxide anions, are commonly used to form room-temperature ionic liquids.[22] The physical, rheological, and chemical properties of POM-ILs can be tuned through chemical design, enabling their application in light-driven water oxidation,[23,24] large-scale petroleum desulfurization,[25] and other technological fields. The synergistic combination of nanomaterials (NMs) and ionic liquids for enhanced extraction efficiency has attracted increasing research interest. Zinc oxide nanoparticles (ZnO NPs) have received considerable attention due to their low toxicity, environmental sustainability, large surface area, and biocompatibility for contaminant detection and analysis,[26] as well as their enhanced stability, simple preparation, and low cost.[27] POM-ILs are thermostable and nonvolatile salts composed of various anions and organic cations with favorable solvation properties that align with green chemistry principles.[28] The combination of POM-ILs with nanomaterials provides higher sorption capacity, improved extraction efficiency, and enhanced sustainability. The extraction performance is significantly improved due to the synergistic effect arising from the material properties.[29]

In this study, a polyoxometalate-based ionic liquid (POM-IL) was synthesized by combining hexadecyltributylphosphonium bromide with the Keplerate-type [Mo_{132}] polyoxometalate and subsequently immobilized onto ZnO nanostructures to fabricate a novel POM-IL@ZnO composite. Although nanoparticle–ionic liquid composites have been widely reported, the integration of a redox-active [Mo_{132}]-based POM-IL with ZnO nanostructures for dispersive micro-solid phase extraction (D-μSPE) of tetracyclines has not been previously reported to the best of our knowledge. This design combines the high surface area and structural stability of ZnO with the tunable charge density and amphiphilic properties of the POM-IL, resulting in a multifunctional sorbent. The synergistic architecture facilitates multiple interaction mechanisms, including electrostatic attraction, hydrogen bonding, and π–π interactions, thereby improving analyte–sorbent affinity. The developed D-μSPE method provides a rapid and environmentally friendly approach for tetracycline determination in water, honey, and milk samples. Overall, this work advances the rational design of POM-IL-based nanocomposites as multifunctional sorbents for antibiotic residue analysis.

2. Materials and methods

2.1. Reagents and materials

Analytical-grade reagents included oxytetracycline (OT, 99%), chlortetracycline (CT, 98.0%), tetracycline (TC, 98.0%), hexadecyltributylphosphonium bromide, zinc nitrate hexahydrate ($Zn(NO_3)_2 \cdot 6H_2O$), hydrazine sulfate ($N_2H_6SO_4$), ammonium acetate (CH_3COONH_4), and ammonium heptamolybdate tetrahydrate ($(NH_4)_6Mo_7O_{24} \cdot 4H_2O$), purchased from Sigma-Aldrich and Merck Life Science Pty Ltd, Bayswater. Stock solutions of OT, TC, and CT were prepared individually in methanol to a final concentration of 1000 mg L^{-1}. Other reagents were stored at 4 °C, while stock standard solutions were stored at −18 °C. Working standard solutions were prepared by appropriate dilution with water before HPLC analysis. All experiments were performed in triplicate unless otherwise stated. Results are presented as mean ± standard deviation (SD). Error bars shown in figures represent the standard deviation of three independent measurements ($n = 3$). Data analysis and plotting were performed using Origin software (Origin Lab, USA).

2.2. Instrumentation

The morphology of the synthesized nanoparticles and composite was examined using a FEI Helios Nanolab G3 CX Dual Beam FIB-SEM (Thermo Fisher Scientific, USA). Crystalline structure was determined using an X-ray diffractometer (D8 Advance, Bruker, Germany). Infrared spectra were recorded using a Fourier-transform infrared (FTIR) spectrometer (Agilent Cary 630, Agilent Technologies, USA) equipped with an attenuated total reflectance (ATR) accessory over the range of 400–4000 cm^{-1}. Thermogravimetric analysis (TGA) was performed using a Q600 analyzer (TA Instruments, USA) by heating 10 mg of sample from 30 to 600 °C at a rate of 10 °C min^{-1} under a nitrogen atmosphere. Chromatographic separation was carried out using a high-performance liquid chromatography system (Shimadzu Corporation, Japan) equipped with a C18 column (4.6 mm, 5 μm; Waters Corporation, USA), an SPD-10A UV detector, and LC-10AT pumps with a CBM-102 system controller and CTO-10A column oven. The mobile phase was delivered at a flow rate of 1.0 mL min^{-1}, and the total run time was 15 min. A 20 μL sample was injected for chromatographic analysis.

2.3. Chromatographic conditions

Tetracycline antibiotics were separated chromatographically using an isocratic mobile phase consisting of 0.01 M oxalic acid in a 70 : 30 (v/v) methanol–water mixture. Separation was performed at a constant flow rate of 1.0 mL min^{-1} on a C18 reversed-phase column (150 mm × 4.6 mm, 5 μm particle size). Detection was carried out using a UV detector set at 360 nm, corresponding to the maximum absorbance of all three tetracycline compounds. The injection volume was 20 μL, and the column temperature was maintained at 30 °C throughout the analysis. The mobile phase was filtered through a 0.22 μm nylon membrane, and all drug samples were filtered using syringe filters before chromatographic analysis.

2.4. Synthesis of Mo_{132} POM

Mo_{132} polyoxometalate (POM) was synthesized using the procedure. Briefly, 5.6 g of $(NH_4)_6Mo_7O_{24}\cdot 4H_2O$ and 12.5 g of ammonium acetate (CH_3COONH_4) were dissolved in 150 mL of deionized (DI) water, followed by the addition of 1 g of hydrazine sulfate ($N_2H_6SO_4$). After 10 min of stirring, the solution turned blue-green. Subsequently, 80 mL of 50% (v/v) acetic acid (CH_3COOH) was added dropwise until the solution turned green. The reaction mixture was left uncovered, and its color gradually changed to brown. After standing for four days, the dark brown mixture was vacuum-filtered. The obtained crystals were washed with ethanol and three times with an ethanol–diethyl ether mixture, followed by vacuum drying to obtain 3.0 g of pure Mo_{132}.

2.5. Synthesis of POM-IL

For the preparation of POM-IL, 2.5 g of Mo_{132} was dissolved in 50 mL of water and heated to 50 °C. In parallel, hexadecyl tributyl phosphonium bromide was dissolved in 80 mL of toluene. The two solutions were combined and vigorously shaken for 24 h to facilitate ion exchange. The resulting dual-phase mixture was allowed to separate, and the organic phase was collected. The solvent was removed under reduced pressure to obtain POM-IL (2.02 g) as a highly viscous liquid. The crude product was purified by washing three times with chloroform and once with toluene to remove unreacted species and residual impurities.

2.6. Synthesis of ZnO NFs

Zinc oxide nanoflowers (ZnO NFs) were prepared using a typical wet chemical reduction method.[30] Briefly, 4.0 g of zinc nitrate hexahydrate [$Zn(NO_3)_2\cdot 6H_2O$] was dissolved in 400 mL of deionized (DI) water in a round-bottom flask and stirred at 50 °C for 10 min to ensure complete dissolution. Subsequently, 3 mL of ammonia solution was added dropwise to initiate crystal formation. The reaction mixture was maintained at 50 °C and allowed to swirl for 24 h. The gradual change of the solution to a milky white color indicated the formation of ZnO nanostructures. The suspension was centrifuged at 6000 rpm for 10 min, and the precipitate was washed with ethanol and DI water to remove residual ions and impurities. The product was then dried at 60 °C in an oven for 12 h. The obtained ZnO was collected as a white powder and stored in a desiccator.

2.7. Synthesis of POM-IL@ZnO

The POM-IL@ZnO composite was prepared by dispersing the synthesized ZnO NFs in an acetonitrile solution of POM-IL. To promote surface interaction and coating, the mixture was vortexed for 10 min. The POM-IL-coated ZnO particles were separated by centrifugation and washed repeatedly with deionized water to remove unattached species. The final product was vacuum-dried at 60 °C for 12 h. The resulting POM-IL-modified nanomaterial was used as the sorbent in the dispersive micro solid-phase extraction (D-μSPE) procedure.

2.8. Real sample preparation

Milk, eggs, and honey samples were purchased from a local supermarket. For milk sample preparation, 2 mL of acetonitrile was added to deproteinize the sample, followed by vortex mixing for 3 min. The mixture was centrifuged at 4000 rpm for 5 min, and the supernatant was collected and filtered through a 0.22 μm syringe filter. The filtrate was diluted with 30 mL of deionized (DI) water before analysis. For honey sample preparation, 4 g of honey was dissolved in 30 mL of deionized water and centrifuged for 2 min. The resulting solution was filtered and used for analysis.

2.9. Spiked samples preparation

Commercially obtained tetracycline standards (TC, OTC, and CTC) were prepared as stock solutions in methanol. The stock solutions were stored in glass vials at 4 °C. Working standard solutions at different concentrations were prepared by serial dilution of the stock solutions with deionized water. For method validation, milk, honey, and water samples were spiked with tetracyclines at concentrations of 5, 15, and 20 μg mL^{-1}. The spiked samples were thoroughly mixed and stored overnight at 4 °C. These samples were then subjected to the dispersive micro solid-phase extraction (D-μSPE) procedure.

2.10. Dispersive micro-solid phase extraction (D-μSPE)

The synthesized POM-IL@ZnO nanocomposite was employed as the adsorbent in D-μSPE under optimized conditions. A 10 mL aliquot of the tetracycline-spiked sample extract was transferred into a 15 mL centrifuge tube, followed by the addition of 10 mg of POM-IL@ZnO. The mixture was vortexed at 5000 rpm for 5 min to ensure efficient dispersion and interaction between the sorbent and analytes. After removal of the supernatant, 1 mL of methanol was added for the desorption of the retained tetracyclines, and the mixture was sonicated for 2 min. The suspension was centrifuged again, and the resulting supernatant was filtered through a 0.22 μm membrane before analysis. The final extract was analyzed using high-performance liquid chromatography with UV detection (HPLC-UV). The synthesis of the ionic liquid composite and the D-μSPE procedure is illustrated in Fig. 1.

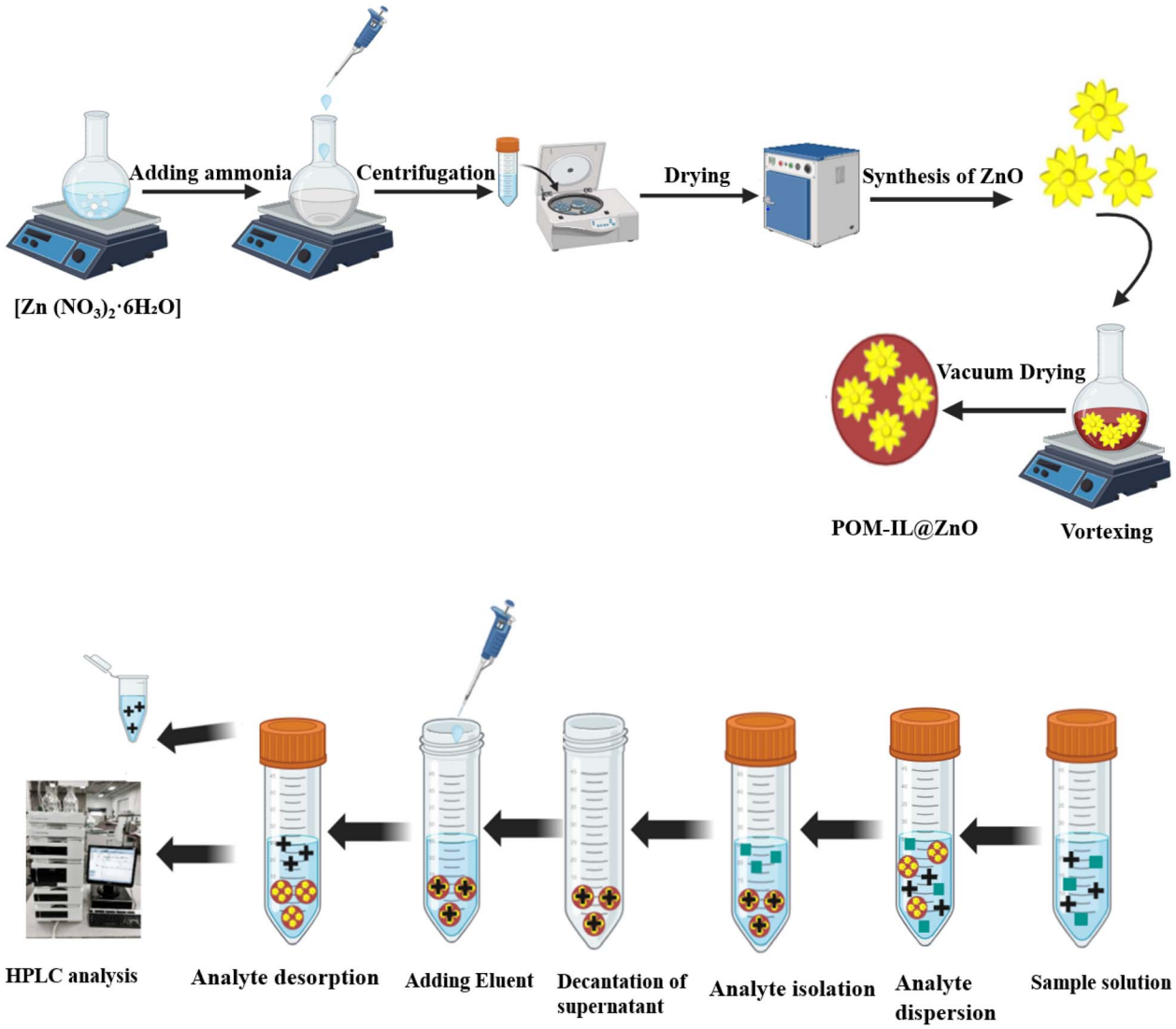

Fig. 1 Schematic depiction of POM-IL@ZnO synthesis and D-μSPE procedures.

3. Results and discussion

3.1. Characterization of POM-IL@ZnO

The structural properties of ZnO, Mo_{132} polyoxometalate-based ionic liquid (POM-IL), and the POM-IL@ZnO composite were investigated using Fourier-transform infrared (FTIR) spectroscopy (Fig. 2). In the ZnO spectrum, a broad absorption band at 3380 cm^{-1} corresponds to O–H stretching vibrations of adsorbed water molecules,[31] while the band at 885 cm^{-1} is attributed to Zn–O stretching vibrations. The POM-IL exhibited characteristic Mo–O vibrational bands at 957, 810, and 707 cm^{-1}, along with C–H stretching bands at 3035 and 2928 cm^{-1}. The band observed at 1470 cm^{-1} is assigned to quaternary ammonium bending vibrations. A band at approximately 1643 cm^{-1} corresponds to H–O–H bending vibrations of residual water molecules associated with ZnO nanoparticles. The POM-IL@ZnO composite demonstrated successful interaction between ZnO and the ionic liquid, as evidenced by the retention of characteristic bands from both components, a shifted Zn–O band at 867 cm^{-1}, C–H stretching bands at 2920 and 2870 cm^{-1}, and an O–H stretching band at 3360 cm^{-1}. The persistence of Mo–O vibrational bands near 803 cm^{-1} confirms the structural stability of Mo_{132} following composite formation. These results verify the successful integration of ZnO and Mo_{132}-based POM-IL into a stable hybrid structure. FTIR analysis confirms strong interactions among ZnO, the polyoxometalate (POM), and the ionic liquid within the POM-IL@ZnO composite. The slight shift of the Mo=O and Mo–O–Mo stretching bands of Mo_{132}, along with changes in the Zn–O vibration region, suggests coordination and hydrogen bonding between surface hydroxyl groups of ZnO and oxygen atoms of the POM framework.

The appearance of C–H stretching bands indicates that the ionic liquid interacts with both the negatively charged POM and the ZnO surface through electrostatic interactions and van der Waals forces. These combined effects create a stable and synergistic interface that enhances electron transfer, dispersion

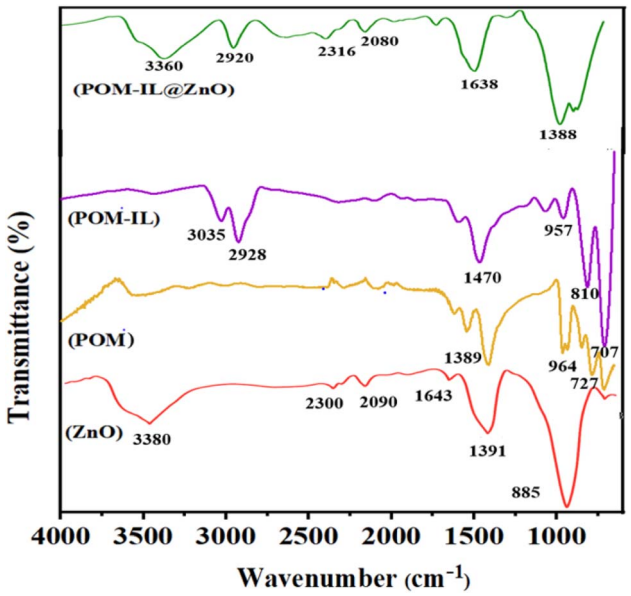

Fig. 2 FTIR spectra of ZnO, POM, POM-IL, and POM-IL@ZnO.

stability, and adsorption efficiency of the composite. Scanning electron microscopy (SEM) was used to examine the morphology of ZnO nanoflowers (NFs) and to verify successful immobilization of the POM-IL coating. The synthesized ZnO NFs exhibited uniformly distributed flower-like structures composed of needle-like multi-branch architectures. Field-emission SEM images (Fig. 3a and b) show that pristine ZnO nanostructures form highly uniform flower-like assemblies consisting of radially oriented nanosheets with dense surface coverage. After functionalization with the ionic liquid (Fig. 3c and d), the hierarchical morphology remained intact; however, smoothing of the surface texture and rounding of nanosheet edges were observed, indicating successful deposition of the ionic liquid layer. It should be noted that POM-IL is a viscous ionic liquid and does not possess a well-defined solid-state morphology suitable for SEM analysis. Therefore, SEM characterization was performed only for ZnO nanoflowers and the POM-IL@ZnO composite to evaluate morphological features and surface modifications following immobilization.

The crystalline structure of ZnO NFs and IL-modified ZnO NFs was identified using a typical PXRD pattern (Fig. 4). All of the different peaks in the ZnO NFs' XRD spectra, which were evaluated using the standard card JCPDS-36-1451, were hexagonal, filamentous ZnO crystals.[32] The PXRD pattern of POM-IL@ZnO closely resembles that of pristine ZnO NFs, indicating that the crystalline structure of ZnO was preserved after ionic liquid modification. These findings confirm the successful synthesis of the POM-IL-functionalized ZnO composite. Retention of the hexagonal ZnO crystal structure after ionic liquid modification indicates that structural integrity and surface stability were maintained, which is essential for preserving adsorption sites during the dispersive micro solid-phase extraction (D-μSPE) process. Although PXRD confirms the crystalline nature of the composite, the material consists of nanostructured polycrystalline domains rather than well-defined single crystals. Therefore, single-crystal X-ray diffraction (SCXRD) analysis was not feasible, and crystallographic features were appropriately evaluated using PXRD. It should be noted that POM-IL, as an ionic liquid, does not exhibit long-range crystalline order; therefore, no crystalline PXRD

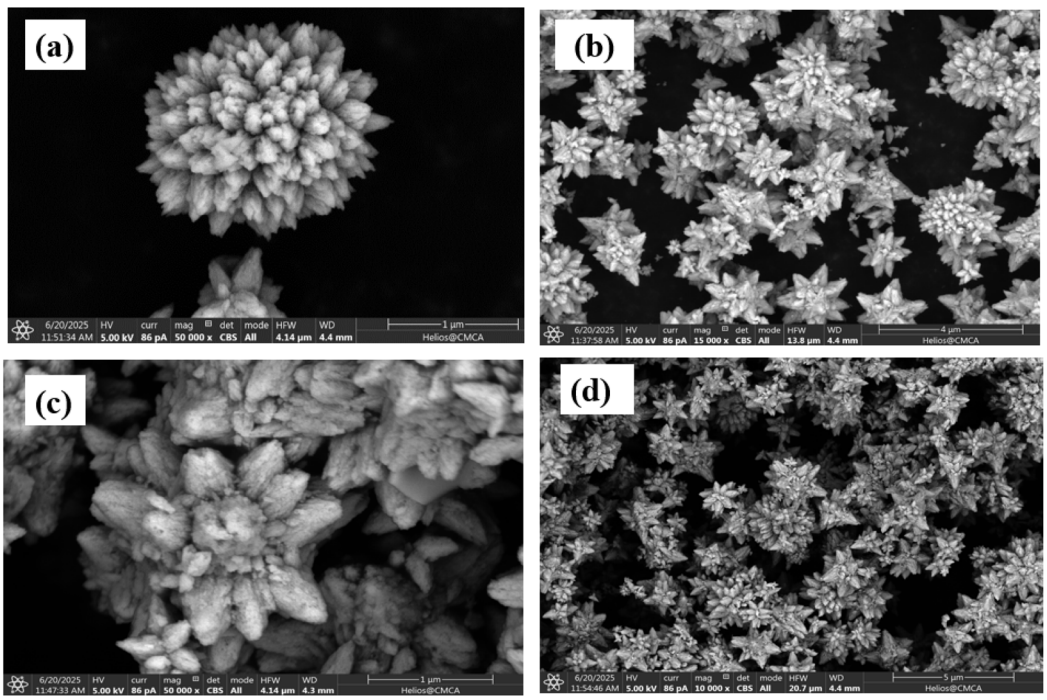

Fig. 3 SEM images of the ZnO nanoflowers (a and b), POM-IL@ZnO (c and d).

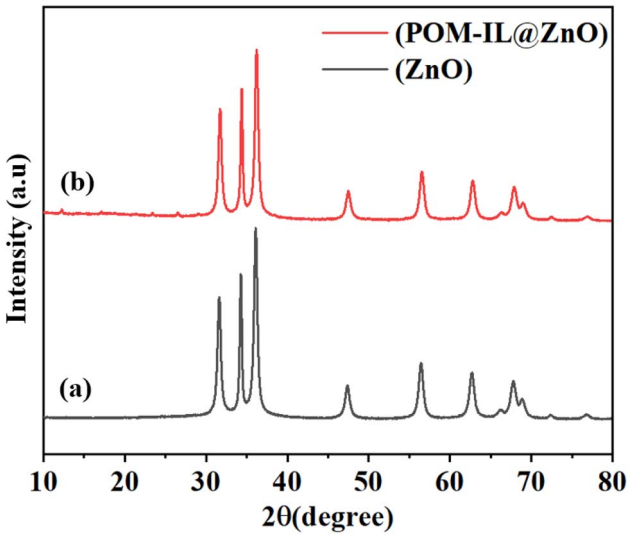

Fig. 4 PXRD patterns of (a) ZnO and (b) POM-IL@ZnO composite indicating crystallinity and composite formation.

reference pattern is expected or available for this component. The absence of POM-derived crystalline peaks in the composite pattern confirms that POM-IL is incorporated as a disordered ionic phase rather than a phase-separated crystalline solid, which is consistent with its ionic liquid nature. The successful incorporation of POM-IL is instead confirmed by FTIR (characteristic Mo–O bands).

The thermal stability of ZnO, POM-IL, and the POM-IL@ZnO composite was evaluated by thermogravimetric analysis (TGA) (Fig. 5). Pure ZnO exhibited negligible weight loss over the investigated temperature range, confirming its inorganic nature and high thermal stability. In contrast, POM-IL displayed a distinct multi-step decomposition profile. The initial weight loss below 150 °C is attributed to the removal of adsorbed moisture and residual solvent. Significant decomposition occurred in the range of 200–450 °C, corresponding to degradation of the Mo_{132} polyoxometalate framework and oxidative decomposition of the hexadecyl tributyl phosphonium cation.[33] In this temperature region, the long alkyl chains of the phosphonium cation undergo oxidative degradation accompanied by cleavage of C–N bonds.[34] The thermal behaviour of the POM-IL@ZnO composite reflects contributions from both constituents. A moderate initial mass loss below 150 °C is associated with moisture removal, similar to that observed for POM-IL. Pronounced mass loss between 200 and 450 °C indicates decomposition of both the POM anion and the organic phosphonium cation. Compared with pure POM-IL, the composite exhibited slightly delayed decomposition and a higher residual mass, demonstrating that immobilization of POM-IL on ZnO enhances thermal stability.

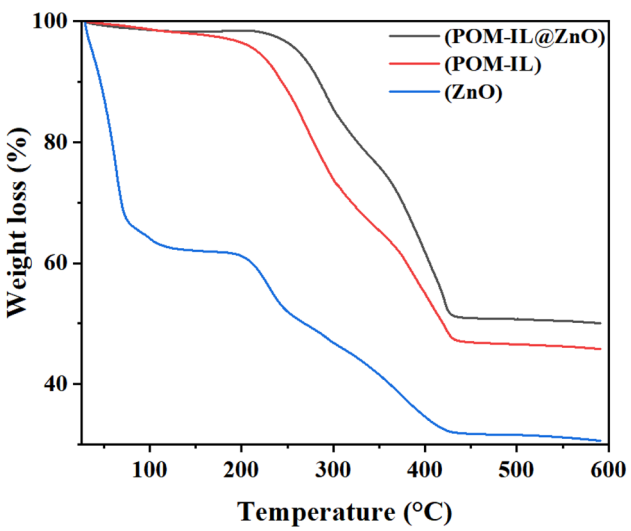

Fig. 5 TGA profiles of ZnO, POM-IL, and POM-IL@ZnO. The composite displays delayed degradation and higher thermal residue compared to the individual components, showing enhanced stability resulting from POM-IL immobilization on the ZnO framework.

The TGA curve becomes stable above 450 °C due to the presence of thermally stable ZnO and residual metal oxide species.[35] Although the overall decomposition profiles of POM-IL and POM-IL@ZnO share similar temperature windows, the composite exhibits a notably higher residual mass, a marginal shift toward higher decomposition onset temperature, and a reduced rate of mass loss in the critical 200–450 °C region. These differences collectively indicate that the thermal degradation pathway is altered upon immobilization, consistent with strong interfacial interaction between POM-IL and the ZnO framework. The thermally stable ZnO component contributes directly to the improved thermal resilience of the composite, supporting its structural integrity during repeated extraction and regeneration cycles. These results confirm that coating ZnO with POM-IL improves overall thermal resistance, which is essential for maintaining structural integrity during extraction and regeneration processes. The high residual mass of POM-IL@ZnO further supports its robustness and suitability for repeated analytical applications.

3.2. Optimization conditions of D-μSPE

The current study thoroughly considered a number of factors that could affect the performance of adsorbents to create an efficient D-μSPE strategy to extract TCs. These were the amount of adsorbent, vortex time, volume of solvent discharged, nature of discharged solvent, pH, and reusability.

3.2.1. Effect of adsorbent amount. In adsorbent-based extraction methods, analytes are separated through adsorption onto active sites of the sorbent material.[36] Increasing the sorbent dosage increases the number of available active sites; therefore, optimization of the adsorbent amount is essential to achieve maximum extraction efficiency. The effect of POM-IL@ZnO dosage was investigated in the range of 2–20 mg. As the sorbent dosage increased, the number of available adsorption sites and effective surface area increased, resulting in enhanced extraction efficiency (Fig. 6a). However, the extraction efficiency reached a plateau at 10 mg, indicating that sufficient active sites were available for analyte binding. Therefore, 10 mg was selected as the optimal adsorbent amount for subsequent experiments.

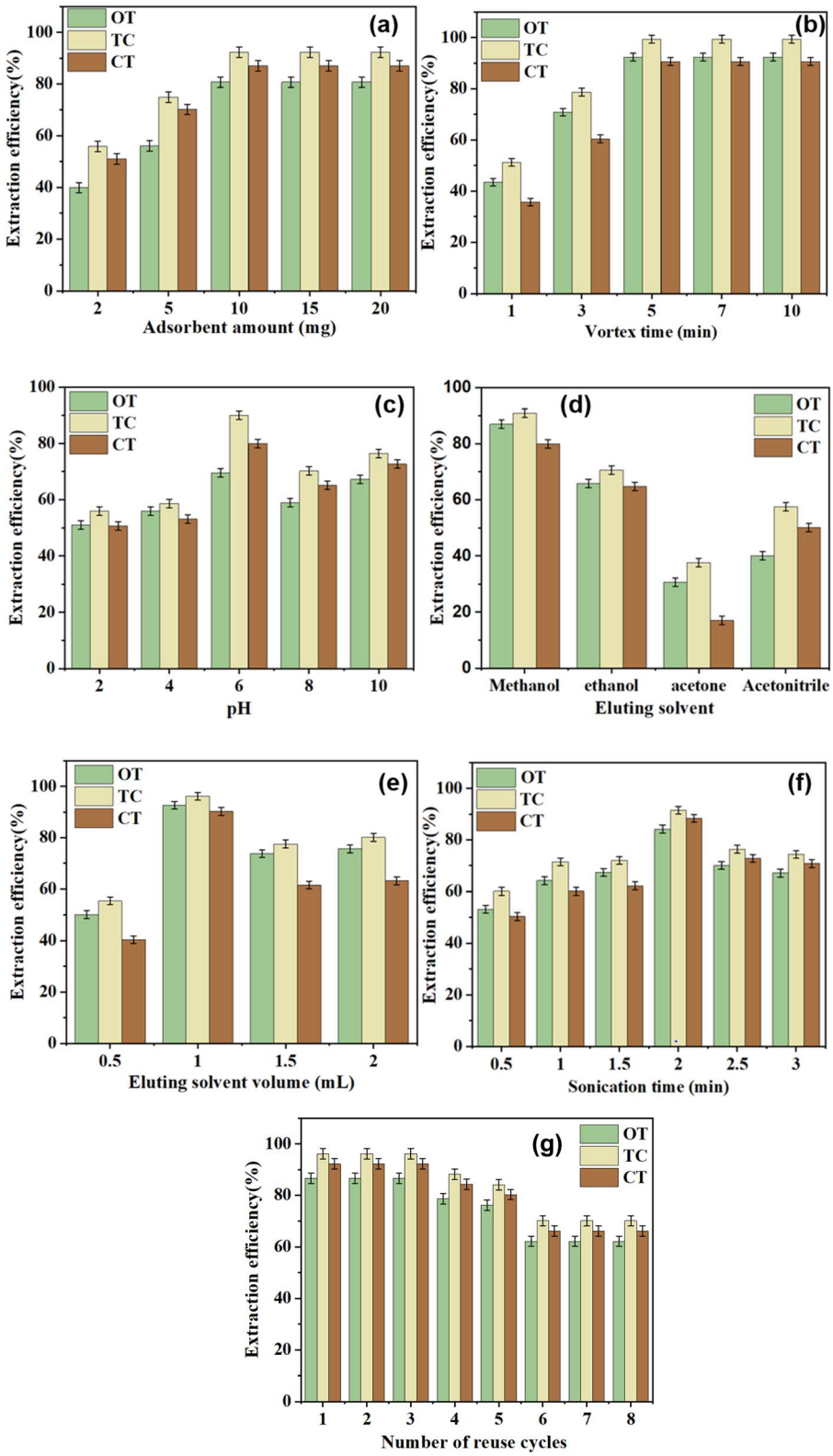

Fig. 6 Effect of the adsorbent amount (a), vortex time (b), pH (c), eluting solvent (d), eluting solvent volume (e), sonication time (f), and number of reuse cycles (g), on the D-μSPE-based extraction efficiency of TCs.

3.2.2. Effect of time. The short diffusion path of nanoparticles enables rapid mass transfer and efficient extraction. Vortex mixing enhances mass transfer during the extraction process.[37] The effect of vortex time on tetracycline adsorption was evaluated in the range of 1–10 min (Fig. 6b). Extraction efficiency increased with vortex time up to 5 min and remained

constant thereafter. Accordingly, 5 min was selected as the optimal vortex time.

3.2.3. Effect of sample pH. The effect of solution pH on adsorption performance is shown in Fig. 6c. Tetracycline adsorption onto Mo_{132} polyoxometalate ionic liquid-functionalized ZnO nanoparticles is strongly pH-dependent due to changes in tetracycline speciation and adsorbent surface charge. Maximum adsorption was observed at pH 6.0, where tetracycline predominantly exists in its zwitterionic form, enabling strong electrostatic interactions, hydrogen bonding, and π–π interactions with the POM-IL@ZnO surface. Under these conditions, the ionic liquid enhances surface functionality, reduces nanoparticle aggregation, and maintains a high density of active sites. At low pH, surface protonation weakens electrostatic interactions, whereas near-neutral conditions favor effective interaction between the adsorbent and tetracycline species. These findings demonstrate the effectiveness of ionic liquid-functionalized ZnO nanoparticles for antibiotic extraction and highlight the critical role of pH in adsorption performance.[38]

3.2.4. The effect of desorption conditions. The efficiency of analyte desorption directly influences the overall extraction efficiency of the sorbent; therefore, optimization of desorption parameters is critical. As shown in Fig. 6d, methanol was more effective than other solvents for eluting tetracyclines from the POM-IL@ZnO sorbent. Selection of the appropriate desorption solvent and volume is essential for the complete recovery of preconcentrated analytes. The desorption performance of ethanol, methanol, acetone, and acetonitrile was evaluated. Methanol exhibited the highest efficiency due to its ability to solubilize tetracyclines and form strong hydrogen bonds with the target molecules. Subsequently, different methanol volumes (0.5–2 mL) were tested, and 1 mL was identified as the optimal volume, yielding the highest recovery efficiency (Fig. 6e). The effect of sonication time on desorption was also investigated. A short sonication duration of 0.5 min resulted in low extraction efficiency, indicating incomplete desorption (Fig. 6f). Increasing the sonication time to 2 min significantly improved recovery. Longer sonication durations led to a slight decrease in efficiency, likely due to adsorption of the analytes onto the centrifuge tube walls.[39] Therefore, 2 min was selected as the optimal sonication time for effective desorption.

3.2.5. Reusability of sorbent. Affordability and accessibility of an adsorbent are closely related to its reusability. The reusability of the POM-IL@ZnO sorbent was evaluated through repeated regeneration cycles. After each extraction run, the sorbent was rinsed three times with methanol and water, followed by sonication. For the dispersive micro solid-phase extraction (D-μSPE) process, the regenerated sorbent was dried at 60 °C for 1 h before reuse. The sorbent maintained effective extraction of tetracyclines (TCs) over eight consecutive cycles, after which a gradual decline in efficiency was observed (Fig. 6g).

3.2.6. Interaction mechanism. The enhanced extraction performance of the POM-IL@ZnO composite can be attributed to the synergistic interaction mechanisms between the sorbent and tetracycline molecules. Tetracyclines possess multiple functional groups, including phenolic hydroxyl, amide, and aromatic rings, which enable diverse interaction pathways. Electrostatic attraction plays a significant role due to the tunable surface charge of the POM-IL component, facilitating interaction with oppositely charged sites of the analytes

Table 1 Analytical performance of the developed method for antibiotics analysis, representing the LOD, LOQ, and linear ranges

Analyte	R^2	Linear range (μg mL^{-1})	LOD (μg mL^{-1})	LOQ (μg mL^{-1})
OT	0.995	10–1000	0.030	0.10
TC	0.991	10–1000	0.026	0.08
CT	0.998	10–1000	0.067	0.21

Table 2 Precision (% RSD) and recovery (% mean ± SD, n = 3) for target analytes at different spiking levels using ZnO and POM-IL@ZnO adsorbents

Adsorbent	Analyte	Spiked level (μg mL^{-1})	Intraday (% RSD)	Interday (% RSD)	% recovery (mean ± SD)	Sample
ZnO	OT	5	4.1	4.9	52 ± 2.1	Honey
		15	3.6	4.3	60 ± 2.6	Milk
		20	3.9	4.5	55 ± 2.5	Water
ZnO	TC	5	3.5	4.8	60 ± 2.4	Honey
		15	4.2	4.1	51 ± 2.1	Milk
		20	4.6	3.3	57 ± 2.3	Water
ZnO	CT	5	4.3	4.2	56 ± 2.3	Honey
		15	4.8	3.1	58 ± 2.4	Milk
		20	3.9	3.7	43 ± 1.9	Water
POM-IL@ZnO	OT	5	2.5	1.3	96.6 ± 1.8	Honey
		15	1.9	2.8	98.2 ± 1.6	Milk
		20	2.6	1.6	99.8 ± 1.5	Water
POM-IL@ZnO	TC	5	1.8	1.4	94.7 ± 1.9	Honey
		15	2.1	2.2	97.9 ± 1.7	Milk
		20	1.5	2.7	97.3 ± 1.8	Water
POM-IL@ZnO	CT	5	1.4	2.1	98.7 ± 1.6	Honey

depending on the solution pH. In addition, hydrogen bonding interactions may occur between the oxygen-containing functional groups of tetracyclines and the oxygen atoms present in the polyoxometalate framework and ZnO surface. Furthermore, π–π interactions between the aromatic rings of tetracyclines and the hydrophobic alkyl chains of the ionic liquid contribute to enhanced adsorption. Importantly, ZnO does not merely serve as a passive support; its surface hydroxyl groups and Lewis acidic Zn^{2+} sites can provide additional adsorption interactions, thereby strengthening analyte binding. The integration of ZnO nanostructures increases accessible surface area, enhances mass transfer, improves dispersion of the ionic liquid phase, and prevents aggregation or leaching of POM-IL. The combined effects of these mechanisms lead to improved analyte–sorbent affinity and extraction efficiency.[40]

3.2.7. Analytical performance of D-μSPE. The performance of the proposed method was evaluated in terms of relative recoveries, limits of detection (LOD), and limits of quantification (LOQ). The LOD and LOQ values were determined based on the signal-to-noise (S/N) criterion, where LOD = 3 × (S/N) and LOQ = 10 × (S/N), using low-concentration standard solutions near the lower limit of the calibration range. Excellent linearity was obtained for the three studies over the concentration range of 10–1000 μg mL^{-1}, with coefficients of determination (R^2) of 0.995, 0.991, and 0.998, respectively. At a signal-to-noise ratio of 3, the calculated LOD values ranged from 0.02 to 0.06 μg mL^{-1}, as summarized in Table 1. Method precision was evaluated using relative standard deviation (RSD), yielding values between 1.8% and 6.0%. The obtained LOD and LOQ values demonstrate the high sensitivity of the proposed D-μSPE-HPLC method, which can be attributed to the enhanced extraction performance of the POM-IL@ZnO composite.

The D-μSPE validation data for TCs from water, milk, and honey samples are displayed in Table 2. It demonstrates that

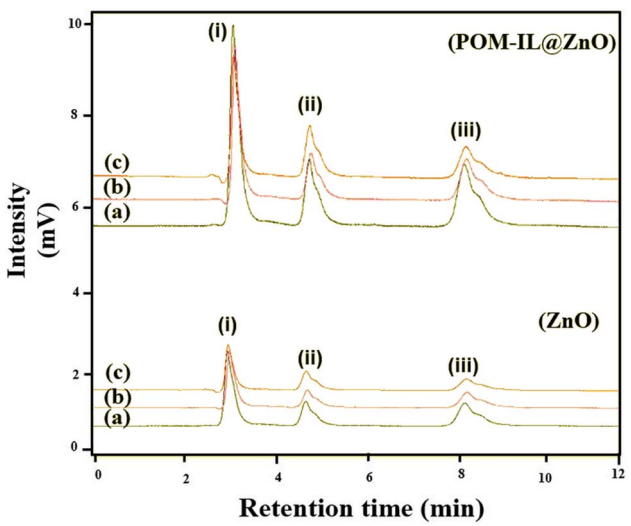

Fig. 7 Comparative HPLC chromatograms of spiked milk (a), honey (b), and water (c) samples extracted using ZnO and POM-IL@ZnO adsorbents. Peaks correspond to (i) oxytetracycline (OT), (ii) tetracycline (TC), and (iii) chlortetracycline (CT).

Table 3 Comparison of the developed method with other methods[a]

Analysis method	Adsorbent	Sample	Detection	Analyte	Linear range (μg L^{-1})	LOD (μg L^{-1})	Recovery (%)	Ref.
MSPE HPLC	Fe_3O_4@MI-POSS	Milk	HPLC-UV	CTC, DC, OTC, TC	10–3000	0.67–8.05	86.2	43
MSPE-DLLME	Fe_3O_4@SiO_2@GO-β-CD	Milk, water	HPLC	Tetracyclines	10–200	1.8–2.9	70.6	44
μ-SPE-HPLC-UV	PET-GO nano-fiber	Honey	HPLC-UV	Tetracycline, cefotaxime	10–5000	15.3	89–94%	45
MISPE HPLC	MIP	Milk	HPLC-UV	Erythromycin, tetracycline, chloramphenicol	20–600	20	81.02–88.17	46
MISPE HPLC	RAM-MMIPs	Milk, egg	HPLC-UV	OT, TC, CT, DC	5.0–700	1.03–1.31	86.7–98.6	47
D-μSPE-HPLC-UV	POM-IL@ZnO	Honey, milk, water	HPLC-UV	OT, TC, CT	10–1000	20–60	99.8	This work

[a] Abbreviations: MSPE-DLLME: magnetic solid phase extraction dispersive liquid–liquid microextraction. μ-SPE-HPLC-UV: micro-solid phase extraction-high-performance liquid chromatography, MISPE HPLC: molecularly imprinted solid-phase extraction coupled with high-performance liquid chromatography, μ-SPE-HPLC-UV: micro-solid-phase extraction coupled with high-performance liquid chromatography-ultraviolet detection, SPE-LC-MS/MS: solid-phase extraction-liquid chromatography-tandem mass spectrometry. RAM-MMIPs: restricted access media-magnetic molecularly imprinted polymers, Fe_3O_4@MI-POSS: Fe_3O_4 nanoparticles molecularly imprinting polyhedral oligomeric silsesquioxanes composites.

good relative recoveries between 60% and 99% were achieved using ZnO and POM-IL@ZnO composite. According to the findings, D-μSPE extraction is a successful method to extract drugs from food and water matrices. The HPLC chromatograms of the OTC, TC, and CT in samples of milk, water, and honey are displayed in Fig. 7. Since the synthesized POM-IL is liquid at room temperature, it is not suitable for direct use in D-μSPE, which requires a solid sorbent material. Therefore, ZnO nanostructures were employed as a solid support to immobilize the POM-IL and enable its practical application in extraction. Consequently, ZnO and POM-IL@ZnO were selected for comparative evaluation to assess the contribution of POM-IL functionalization to the overall extraction performance.

3.3. Comparison with reported studies

This study presents a novel dispersive micro solid-phase extraction (D-μSPE) method for the determination of tetracyclines (TCs) in food and water samples using ionic liquid (IL)-functionalized ZnO nanoflowers (NFs). The method was compared with previously reported techniques, as summarized in Table 3, encompassing key analytical parameters including extraction sorbent, sample matrix, analyte type, detection method, analysis method, linear range, LOD, recovery (%), to provide a comprehensive and balanced evaluation. To the best of our knowledge, this is the first application of D-μSPE using a POM-IL@ZnO composite for the analysis of TCs in milk, honey, and water. The use of a novel POM-IL@ZnO composite sorbent not previously applied in D-μSPE of tetracyclines; (ii) simple, rapid, and reagent-efficient extraction procedure; (iii) applicability without specialized instrumentation; and (iv) cost-effective and reusable sorbent. Conventional solid-phase extraction (SPE) procedures often require large volumes of organic solvents and sorbents, making them expensive, labor-intensive, and time-consuming.[41] In contrast, the D-μSPE method is more efficient, requiring smaller volumes of solvents and sorbent material for each analysis. Moreover, it is cost-effective, simple, and suitable for routine applications, as it only requires basic laboratory equipment, such as a centrifuge and sonicator. Functionalization of nanoparticles with ionic liquids further enhances the method's advantages by improving environmental compatibility, owing to their low toxicity and eco-friendliness.[42]

4. Conclusion

This study presents a practical analytical method for the determination of three tetracyclines (TCs) in food and water samples using a polyoxometalate ionic liquid-functionalized zinc oxide composite (POM-IL@ZnO) as a sorbent in dispersive micro-solid phase extraction (D-μSPE). Key parameters affecting adsorption and desorption were systematically optimized to achieve reliable analytical performance. The developed method demonstrated satisfactory sensitivity, precision, and applicability for the analysis of complex sample matrices. The enhanced extraction performance can be attributed to the synergistic integration of ZnO nanostructures with the polyoxometalate-based ionic liquid, which strengthens analyte–sorbent interactions. Moreover, the POM-IL@ZnO composite was easy to synthesize, cost-effective, and reusable with good stability, supporting its practical applicability. Despite these promising results, the present study was limited to selected tetracyclines and specific sample matrices. Further investigation is required to evaluate the applicability of the composite toward a broader range of antibiotics and emerging contaminants, as well as to assess long-term stability under varied environmental conditions. Future studies may also explore surface modification strategies, deeper mechanistic investigations, and scale-up approaches to enhance practical implementation. Overall, this work provides a foundation for the rational design of POM-IL-based nanocomposites as multifunctional sorbents for advanced analytical applications.

Author contributions

Zahra Nazar: methodology, data curation, software, formal analysis, writing – original draft review & editing. Mohannad Al-Hmoud: data curation, formal analysis, writing – original draft review & editing. Zahra Mohammadizadeh Tahroudi: data curation, software, formal analysis, writing – original draft review & editing. Alexandra Suvorova: data curation, software, formal analysis, writing – original draft review & editing. Muhammad Salman Khan: conceptualization, data curation, formal analysis, writing – original draft review & editing. Ayed M. Binzowaimil: data curation, formal analysis, writing – original draft review & editing. Hijaz Ahmad: data curation, formal analysis, writing – original draft review & editing. Ahmad Irfan: data curation, formal analysis, writing – original draft review & editing.

Conflicts of interest

The authors have no conflicts interest.

Data availability

Data are available upon request from the corresponding author.

Acknowledgements

This work was supported and funded by the Deanship of Scientific Research at Imam Mohammad Ibn Saud Islamic University (IMSIU) (grant number IMSIU-DDRSP2601).

References

1 H. Huang, L. Wanxiang, Y. Wanxiang, G. Xiaojing, H. Yejing, Z. Qing and Z. Haiyun, *Microchem. J.*, 2019, **150**, 104097.
2 J. Scaria, K. V. Anupama and P. V. Nidheesh, *Sci. Total Environ.*, 2021, **771**, 145291.
3 Y. Zhou, H. Liu, J. Li, Z. Sun, T. Cai, X. Wang, S. Zhao and B. Gong, *J. Chromatogr. A*, 2020, **1613**, 460684.
4 N. Gissawong, S. Boonchiangma, S. Mukdasai and S. Srijaranai, *Talanta*, 2019, **200**, 203–211.

5 N. Cini and A. Gölcü, *Curr. Anal. Chem.*, 2021, **17**, 1141–1168.
6 L. Lian, J. Lv, X. Wang and D. Lou, *J. Chromatogr. A*, 2018, **1534**, 1–9.
7 S. M. Taghdisi, N. M. Danesh, M. Ramezani and K. Abnous, *Biosens. Bioelectron.*, 2016, **85**, 509–514.
8 M. Shirani, M. Faraji, H. Rashidi Nodeh, B. Akbari-Adergani and S. Sepahi, *J. Food Sci. Technol.*, 2023, **60**, 2802–2812.
9 L. D. Nguyen, N. H. Nguyen, M. H. N. Do, T. T. Nguyen, T. H. Nguyen, C. T. G. Hua and P. H. Tran, *Microchem. J.*, 2024, **204**, 110999.
10 N. Al-Afy, H. Sereshti, A. Hijazi and H. Rashidi Nodeh, *J. Chromatogr. B*, 2018, **1092**, 480–488.
11 H.-Z. Tang, Y.-H. Wang, S. Li, J. Wu, Z.-X. Gao and H.-Y. Zhou, *J. Food Sci. Technol.*, 2020, **57**, 2884–2893.
12 P. Li, D. Rao, Y. Wang and X. Hu, *Microchem. J.*, 2022, **173**, 106935.
13 Z.-M. Dong, L. Cheng, T. Sun, G.-C. Zhao and X. Kan, *Microchim. Acta*, 2021, **188**, 43.
14 G. Li and K. H. Row, *J. Sep. Sci.*, 2022, **45**, 883–895.
15 E. Caro, R. M. Marcé, P. A. G. Cormack, D. C. Sherrington and F. Borrull, *Anal. Chim. Acta*, 2005, **552**, 81–86.
16 B. Arabsorkhi and H. Sereshti, *Microchem. J.*, 2018, **140**, 241–247.
17 F. Yu, J. Ma and S. Han, *Sci. Rep.*, 2014, **4**, 5326.
18 A. Amiri, F. Ghaemi and B. Maleki, *Microchim. Acta*, 2019, **186**, 131.
19 S.-S. Wang and G.-Y. Yang, *Chem. Rev.*, 2015, **115**, 4893–4962.
20 M. T. Pope and A. Müller, *Angew. Chem., Int. Ed.*, 1991, **30**, 34–48.
21 A. V. Anyushin, A. Kondinski and T. N. Parac-Vogt, *Chem. Soc. Rev.*, 2020, **49**, 382–432.
22 P. G. Rickert, M. R. Antonio, M. A. Firestone, K.-A. Kubatko, T. Szreder, J. F. Wishart and M. L. Dietz, *J. Phys. Chem. B*, 2007, **111**, 4685–4692.
23 J. Chen, H. Li, W. Zhu, R. Zhang, L. Guo, C. Chen, H. Gan, B. Song and Z. Hou, *Catal. Commun.*, 2014, **47**, 18–21.
24 G. Bernardini, A. G. Wedd, C. Zhao and A. M. Bond, *Proc. Natl. Acad. Sci. U. S. A.*, 2012, **109**, 11552–11557.
25 W. Huang, W. Zhu, H. Li, H. Shi, G. Zhu, H. Liu and G. Chen, *Ind. Eng. Chem. Res.*, 2010, **49**, 8998–9003.
26 S. Arya, P. Mahajan, S. Mahajan, A. Khosla, R. Datt, V. Gupta, S.-J. Young and S. K. Oruganti, *ECS J. Solid State Sci. Technol.*, 2021, **10**, 023002.
27 S. Arya, P. K. Lehana and S. B. Rana, *J. Electron. Mater.*, 2017, **46**, 4604–4611.
28 S. V. Burov and A. K. Shchekin, *J. Chem. Phys.*, 2010, **133**, 244109.
29 P. Zhou, R. Wang, R. Fan, X. Yang, H. Mei, H. Chen, H. Wang, Z. Wang and X. Wang, *Ecotoxicol. Environ. Saf.*, 2021, **222**, 112482.
30 T. Jiao, F. Y. H. Kutsanedzie, J. Xu, A. Viswadevarayalu, M. M. Hassan, H. Li, Y. Xu and Q. Chen, *Phys. Lett. A*, 2019, **383**, 1312–1317.
31 M. Ghosh, N. Dilawar, A. K. Bandyopadhyay and A. K. Raychaudhuri, *J. Appl. Phys.*, 2009, **106**, 084306.
32 P. Arya, S. Arya, A. Sharma, B. Singh, A. Tomar, S. Singh and R. Sharma, *Integr. Ferroelectr.*, 2020, **205**, 1–13.
33 F. Heym, W. Korth, J. Thiessen, C. Kern and A. Jess, *Chem. Ing. Tech.*, 2015, **87**, 791–802.
34 S. F. Kurtoğlu-Öztulum, A. Jalal and A. Uzun, *J. Mol. Liq.*, 2022, **363**, 119804.
35 N. V. Maksimchuk and O. A. Kholdeeva, *Catalysts*, 2023, **13**, 360.
36 M. Ghorbani, M. Aghamohammadhassan, H. Ghorbani and A. Zabihi, *Microchem. J.*, 2020, **158**, 105250.
37 Y.-P. Gao, Y. Yang, L. Li, W.-J. Wei, H. Xu, Q. Wang and Y.-Q. Qiu, *Anal. Chim. Acta*, 2020, **1110**, 72–81.
38 M. S. Goda, N. Shehata, M. H. Shaltout and A. Zaher, *ChemistrySelect*, 2025, **10**, e05432.
39 J. Zhao, Y. Zhu, Y. Jiao, J. Ning and Y. Yang, *J. Sep. Sci.*, 2016, **39**, 3789–3797.
40 A. Zhu, Y. Zhang, J. Wang, Y. Liu, H. Li and H. He, *Food Chem.*, 2022, **391**, 133277.
41 A. Wilkowska and M. Biziuk, *Food Chem.*, 2011, **125**, 803–812.
42 D. Afzali, M. Ghanbarian, A. Mostafavi, T. Shamspur and S. Ghaseminezhad, *J. Chromatogr. A*, 2012, **1247**, 35–41.
43 R. Peng, Z. Zhou, Q. Wang, Q. Yu, X. Yan, H. Qin, Y. Lei, H. He and L. Luo, *J. Chromatogr. A*, 2019, **1597**, 28–38.
44 N. Al-Afy, H. Sereshti, A. Hijazi and H. Rashidi Nodeh, *J. Chromatogr. B*, 2018, **1092**, 480–488.
45 B. Arabsorkhi and H. Sereshti, *Microchem. J.*, 2018, **140**, 241–247.
46 Y. Xie, Q. Hu, M. Zhao, Y. Cheng, Y. Guo, H. Qian and W. Yao, *Food Anal. Methods*, 2018, **11**, 374–381.
47 Y. Zhou, H. Liu, J. Li, Z. Sun, T. Cai, X. Wang, S. Zhao and B. Gong, *J. Chromatogr. A*, 2020, **1613**, 460684.